Journal of Magnetic Resonance 212 (2011) 149–153

Contents lists available at ScienceDirect

Journal of Magnetic Resonance

journal homepage: www.elsevier.com/locate/jmr

Zeeman shift – A tool for assignment of ^{14}N NQR lines of nonequivalent ^{14}N atoms in powder samples

J. Luznik [a], V. Jazbinsek [a], J. Pirnat [a], J. Seliger [b], Z. Trontelj [a,*]

[a] Institute of Mathematics, Physics and Mechanics, Jadranska 19, 1000 Ljubljana, Slovenia
[b] J. Stefan Institute, Jamova 39, 1000 Ljubljana, Slovenia

ARTICLE INFO

Article history:
Received 10 February 2011
Revised 30 May 2011
Available online 1 July 2011

Keywords:
Zeeman perturbed NQR
Line shapes in powder samples

ABSTRACT

The use of Zeeman perturbed ^{14}N nuclear quadrupole resonance (NQR) to determine the ν_+ and ν_- ^{14}N lines in polycrystalline samples with several nonequivalent nitrogen atoms was investigated. The ^{14}N NQR line shift due to a weak external Zeeman magnetic field was calculated, assuming isotropic distribution of EFG tensor directions. We calculated the broad line distribution of the ν_+ and ν_- line shifts and experimentally confirmed the calculated Zeeman field dependence of singularities (NQR peaks) in cyclotrimethylenetrinitramine (RDX) and aminotetrazole monohydrate (ATMH). The calculated and measured frequency shifts agreed well. The proposed measurement method enabled determination of which ^{14}N NQR lines in ATMH belong to ν_+ and which to ν_- transitions.

1. Introduction

The nuclear quadrupolar interaction is described in the presence of a small external magnetic field by a two term Hamiltonian: the leading quadrupolar term and the perturbing Zeeman term.

$$H = H_Q + H_Z \tag{1}$$

For the case of spin $I = 1$ ^{14}N nuclei with $\eta \neq 0$, the leading term gives three energy levels and three allowed transitions with the corresponding frequencies [1,2] shown in Fig. 1:

$$\nu_+ = \frac{3e^2qQ}{4h}\left(1+\frac{\eta}{3}\right), \quad \nu_- = \frac{3e^2qQ}{4h}\left(1-\frac{\eta}{3}\right) \quad \text{and} \quad \nu_0 = \frac{e^2qQ}{2h}\eta \tag{2}$$

Here e^2qQ/h is the quadrupole coupling constant Q_{cc}, $eq = V_{zz}$ is maximal component of the electric field gradient tensor, eQ is nuclear quadrupole moment and $\eta = (V_{xx} - V_{yy})/V_{zz}$ is asymmetry parameter.

Several analyses of the influence of Zeeman magnetic field on pure NQR resonance lines were made [3–7]. In the presence of a small Zeeman magnetic field B and with a ^{14}N Larmor frequency $\nu_L = \gamma B/2\pi \ll \nu_0$, the second-order perturbation theory gives a new set of transition frequencies [7,8]:

$$\begin{aligned}
\nu_+^* &= \nu_+ + \frac{4\nu_L^2}{Q_{cc}}\left(\frac{2\sin^2\theta\cos^2\phi}{3+\eta} + \frac{\sin^2\theta\sin^2\phi}{3-\eta} + \frac{\cos^2\theta}{2\eta}\right) \\
&= \nu_+ + \frac{4\nu_L^2}{Q_{cc}} f_+(\theta,\phi,\eta) \\
\nu_-^* &= \nu_- + \frac{4\nu_L^2}{Q_{cc}}\left(\frac{\sin^2\theta\cos^2\phi}{3+\eta} + \frac{2\sin^2\theta\sin^2\phi}{3-\eta} - \frac{\cos^2\theta}{2\eta}\right) \\
&= \nu_- + \frac{4\nu_L^2}{Q_{cc}} f_-(\theta,\phi,\eta) \\
\nu_0^* &= \nu_0 + \frac{4\nu_L^2}{Q_{cc}}\left(\frac{\sin^2\theta\cos^2\phi}{3+\eta} - \frac{\sin^2\theta\sin^2\phi}{3-\eta} + \frac{\cos^2\theta}{\eta}\right) \\
&= \nu_0 + \frac{4\nu_L^2}{Q_{cc}} f_0(\theta,\phi,\eta)
\end{aligned} \tag{3}$$

Here θ is the angle between the Zeeman magnetic field and the principal Z-axis of the EFG tensor and ϕ is corresponding azimuthal angle. These transition frequencies are sample orientation dependent and this dependence can be well observed in a single crystal measurement. It is not always clear to which transitions belong the measured NQR lines. The aim of this research was to obtain an improvement in identification of measured NQR transition frequencies. In polycrystalline (powder) samples, which we usually have when identifying illicit substances or studying polymorphism, the orientations of the EFG tensor are randomly distributed. To calculate the line shape(s) for a powder sample, we assume an isotropic distribution of the EFG tensor directions, i.e. homogeneous distribution of $\cos\theta$ and ϕ values in the $(\cos\theta, \phi)$ plane:

$$\frac{1}{N}\frac{dN}{d\Omega} = \frac{1}{N}\frac{dN}{d(\cos\theta)d\phi} = \frac{1}{4\pi} \tag{4}$$

* Corresponding author. Address: IMFM, Jadranska 19, 1000 Ljubljana, Slovenia. Fax: +386 1 2517281.
E-mail address: zvonko.trontelj@fmf.uni-lj.si (Z. Trontelj).

1090-7807/$ - see front matter © 2011 Elsevier Inc. All rights reserved.
doi:10.1016/j.jmr.2011.06.023

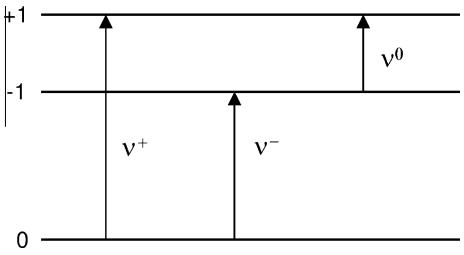

Fig. 1. Quadrupole energy levels and allowed transitions for a spin 1 nucleus.

N is here the total number of nuclei contributing to the observed signal distribution. In calculating the powder line shape we limit ourselves to the ν_+ and ν_- lines. The ν_0 transition lines are at present less important since they are given by the difference of the ν_+ and ν_- lines, as in the unperturbed case. The $f_+(\theta,\phi,\eta)$ and $f_-(\theta,\phi,\eta)$ dependences in expression (3) can be graphically represented in the $(\cos\theta,\ \phi)$ plane as lines of equal frequency shift p_+ for ν_+ and p_- for ν_- lines:

$$f_+(\theta,\phi,\eta)=p_+ \quad \text{and} \quad f_-(\theta,\phi,\eta)=p_- \tag{5}$$

From (3) and (5) we can obtain a suitable expression which enables us to draw a map of the lines of equal frequency shift $p_\pm$:

$$\cos\theta_+(\phi,\eta,p_+)=\sqrt{\frac{p_+-2\cos 2\phi/(3+\eta)-\sin^2\phi/(3-\eta)}{1/2\eta-2\cos^2\phi/(3+\eta)-\sin^2\phi/(3-\eta)}}$$
$$\cos\theta_-(\phi,\eta,p_-)=\sqrt{\frac{p_--\cos^2\phi/(3+\eta)-2\sin^2\phi/(3-\eta)}{-1/2\eta-\cos^2\phi/(3+\eta)-2\sin^2\phi/(3-\eta)}} \tag{6}$$

A typical example for $\eta=0.5$ is shown in Fig. 2. Because of the isotropic distribution of EFG orientations in the $(\cos\theta,\ \phi)$ plane, the contribution to the broadened NQR signal with a certain frequency shift $p_\pm$ is proportional to the area $dS_\pm(p_\pm)$ of the band between two consecutive lines $p_\pm$ and $p_\pm+dp_\pm$. The contribution of all relevant quadrupole nuclei in a sample to the NQR signal is maximal where the area between two consecutive $p_\pm$ – lines of equal frequency shift in Fig. 2 is maximal, i.e. for the values of $p_\pm$ on the line inside the designated band in Fig. 2. It is evident that the points at $\phi=0,\ \pi,\ 2\pi$ and $\cos\theta=0$ belong to the layer contributing to the maxima in the intensity of the ν_+ and ν_- lines. The maximum for the ν_+ line is at $p_+=2/(3+\eta)$ and for the ν_- line at $p_-=1/(3+\eta)$ given by the following expression:

$$(\nu_+^*)_{\max}=\nu_+ +\frac{4\nu_L^2}{Q_{cc}}\frac{2}{3+\eta} \quad (\nu_-^*)_{\max}=\nu_- +\frac{4\nu_L^2}{Q_{cc}}\frac{1}{3+\eta} \tag{7}$$

The dependence of band area on p is obtained by calculating the integrals $\int_0^{2\pi} d(\cos\theta_+(\phi,\eta,p_+))d\phi$ and $\int_0^{2\pi} d(\cos\theta_-(\phi,\eta,p_-))d\phi$

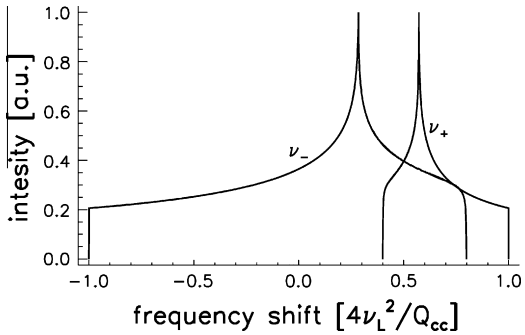

Fig. 3. The calculated broad ^{14}N line shapes (for ν_+ and ν_- ^{14}N NQR resonance lines) for $\eta=0.5$ in a powder sample subjected to a weak Zeeman field.

$$I_+(\eta,p_+)=\frac{1}{N}\frac{dN(p_+)}{dp}=\frac{1}{4\pi}\int_0^{2\pi}\frac{d(\cos\vartheta_+)}{dp}d\phi$$
$$I_-(\eta,p_-)\ =\frac{1}{N}\frac{dN(p_-)}{dp}=\frac{1}{4\pi}\int_0^{2\pi}\frac{d(\cos\vartheta_-)}{dp}d\phi \tag{8}$$

Considering (3) and calculating the expressions for $I_+(\eta,p_+)$ and $I_-(\eta,p_-)$ enabled us to obtain the ν_+ and ν_- line shapes. The calculated shapes of the ν_+ and ν_- lines for $\eta=0.5$ in a powder sample is shown in Fig. 3. The natural NQR line widths are not considered in this presentation. Distinct, measurable differences in the ν_+ and ν_- line shifts distributions can be used for NQR line characterization.

The shift of maximum of the ν_+ line is twice as large as that of the ν_- line. Also the ν_+ line is much narrower than the ν_- line. The broadening for the ν_- line is greater than that for the ν_+ line because the defined values of parameter p_+ are $p_+\in\left[\frac{1}{3-\eta},\frac{1}{2\eta}\right]$ for the ν_+ line and $p_-\in\left[-\frac{1}{2\eta},\frac{2}{3-\eta}\right]$ for the ν_- line. Consequently, the ν_- line experiences a faster decrease in intensity when the Zeeman field is applied. In Figs. 2 and 3 we present the case for $\eta=0.5$. For smaller η values similar dependences of transition frequency shifts are obtained, as long as the condition $\nu_L=\gamma B/2\pi\ll\nu_0$ is fulfilled, except that the broadenings of the shifted lines are stronger, as follows from the allowed value of parameter p. (For $\eta=0$ when $\nu_+=\nu_-$ there is no frequency shift, only symmetric broadening proportional to ν_L appears.). The opposite is true for higher η values where the broadening of the shifted lines is smaller. For instance for $\eta=1$ there is no broadening for the ν_+ NQR transition line. It is only shifted to higher frequencies. However, for the ν_- line the broadening still takes place.

In the above approximation we assumed that the sample response to the RF excitation is also isotropic. That could be achieved by the use of a large sample in a coil of length shorter than its diameter. In this coil the RF excitation directions are strongly spatially dependent. Normally, we take into account the EFG tensor orientations with its x-axis for the ν_+ and y-axis for the ν_- transitions parallel to the RF excitation as privileged in the

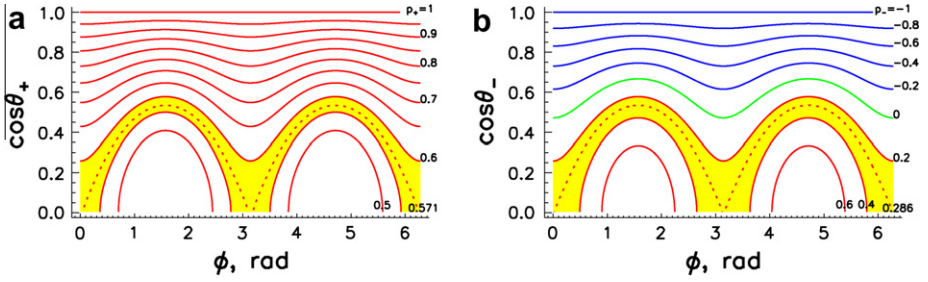

Fig. 2. Lines of equal frequency shift of ν_+ (panel a) and ν_- (panel b) transitions for $\eta=0.5$. The band with maximal area between two neighboring lines of equal frequency shift is shaded.

detection efficiency. Consequently, the NQR line shape depends on the angle between Zeeman and RF field orientation. The two extreme situations are: RF field parallel and RF field perpendicular to Zeeman field.

The contribution of nuclei with different orientations to the signal intensity is proportional to the cosine square of the angle between RF field and principal x-axis of the EFG tensor for the ν_+ transitions (y-axis for the ν_- transitions). This can be included into the calculation of the line shape. When RF field is parallel with Zeeman field, mainly the nuclei with orientations $\cos\theta = 0$ for the ν_+ and ν_- transitions are excited. Contributions of nuclei with other orientations are proportional to $\cos^2(\theta - \pi/2) = \sin^2\theta$. The expected line shapes can be calculated also in this case. We have to consider the integrals:

$$I_+(\eta, p_+) \propto \frac{1}{4\pi}\int_0^{2\pi} \frac{d(\cos\vartheta_+)}{dp}\sin^2\vartheta_+ d\phi \quad \text{and}$$
$$I_-(\eta, p_-) \propto \frac{1}{4\pi}\int_0^{2\pi} \frac{d(\cos\vartheta_-)}{dp}\sin^2\vartheta_- d\phi \qquad (9)$$

The calculated line shape is shown in Fig. 4a. Similarly, the angular dependence can be included in a line shape calculation also for the orientation of RF field perpendicular to Zeeman field with $\sin^2\phi$ for the ν_+ and $\cos^2\phi$ for the ν_- transition dependences:

$$I_+(\eta, p_+) \propto \frac{1}{4\pi}\int_0^{2\pi} \frac{d(\cos\vartheta_+)}{dp}\sin^2\phi\, d\phi \quad \text{and}$$
$$I_-(\eta, p_-) \propto \frac{1}{4\pi}\int_0^{2\pi} \frac{d(\cos\vartheta_-)}{dp}\cos^2\phi\, d\phi$$

The result is shown in Fig. 4b.

It can be seen (Fig. 4) that the expected shifts for both lines are limited with the intervals $f_+ \in [0.4, 1]$ for the ν_+ and $f_- \in [-1, 0.8]$ for the ν_- transitions. Maxima of the intensity are expected at 0.57 for the ν_+ and at 0.29 for the ν_- transition lines. Usually, the frequency shifts are only a few natural line widths, because for higher Zeeman fields the decrease in the intensity of both lines is too strong and the signals cannot be observed. With standard measurements we ordinary cannot see the exact structures of the shifted lines, but only a superposition of natural broadening and frequency shifts, manifesting as very broad lines around centers of gravity (Fig. 4). It is evident that for the orientation with RF and Zeeman field being parallel a rather small difference of shifts for the ν_+ and ν_- lines causes difficult resolution of both lines. Opposite is true for perpendicular orientation of the two fields where the ν_- line is less shifted towards the higher frequency and the difference in shift between both lines can be observed easier. To see experimentally the difference between the ν_+ and ν_- lines a perpendicular orientation of RF and Zeeman field is recommended.

2. Experimental

Our first experiments were performed with the explosive RDX ($C_3H_6N_6O_6$). Here there are three sets of ν_+, ν_- and ν_0 transition frequencies for the three different ring positions of ^{14}N nuclei in the molecule [9,10]. We chose RDX because it gives very well resolved ^{14}N NQR spectra in a short measuring time. The data for the ^{14}N NQR transition frequencies are collected in Table 1.

For all three sets of lines the asymmetry parameter $\eta \sim 0.6$ and the quadrupole coupling constant Q_{cc} is between 5600 kHz and 5800 kHz. In a Zeeman magnetic field $B \sim 20$ mT we expect from (7) frequency shifts of around 1400 Hz and 700 Hz for the ν_+ and ν_- lines, respectively. The calculated values are in good agreement with our experimental results (Table 1).

With longer averaging we can get in RDX sufficiently well resolved signals also in the presence of Zeeman magnetic field. The influence of a 25 mT magnetic field on middle pair of the ν_+, ν_- transition lines (5191 kHz, 3410 kHz), obtained after a long averaging (100.000 averages) is shown in Fig. 5. Not only the shifts, but also the structures of the shifted lines can be seen. Comparing shapes of the measured and calculated lines (Fig. 5) a good agreement can be clearly observed. The shift of ν_- line is smaller and the line is asymmetrically broadened towards lower frequency from the peak value. For ν_+ line the shift is bigger and the line is asymmetrically broadened towards higher frequency. From Fig. 5 we can see that the calculated shifts at 25 mT are $\Delta\nu_+ = 2500$ Hz and $\Delta\nu_- = 1200$ Hz. From Table 1 we see that the measured shifts at 20 mT are 1500 Hz and 750 Hz. Considering the B^2 dependence of shifts, the agreement is good. Because of geometrical constraints in our Zeeman field generator only measurements with perpendicular orientation of RF and Zeeman field could be completed.

We also measured the orientation dependence of RF field on Zeeman field, however, with lower resolution. That means the measured RDX sample was small (15 mm, 7 mm diameter). It was placed in the middle of 25 mm solenoid RF coil. This RF coil enabled a complete rotation in the volume of constant Zeeman field generated by an electromagnet. We measured the angular dependence of frequency shift and line broadening in a constant Zeeman field of around 25 mT for the ν_+ and ν_- transition lines. The average frequency shift and broadening for all three ν_- lines

Table 1
Measured RDX ^{14}N NQR transition frequencies ν_+ and ν_-, asymmetry parameters, quadrupole coupling constants and frequency shifts $\Delta\nu_+$ and $\Delta\nu_-$ in a 20 mT (200 Gauss) Zeeman magnetic field oriented perpendicular to the RF field (all at 298 K).

ν_+ (kHz)	ν_- (kHz)	ν_0 (kHz)	η	Q_{cc} (kHz)	$\Delta\nu_+$ (Hz)	$\Delta\nu_-$ (Hz)
5239	3458	1781	0.61	5800	1400	700
5191	3410	1781	0.62	5735	1500	750
5046	3359	1687	0.60	5605	1500	750

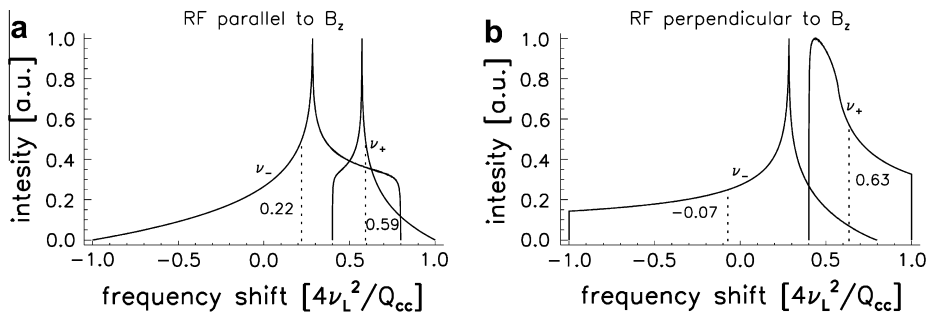

Fig. 4. The calculated line shapes for the NQR ν_+ and ν_- transitions, as well as their centers of gravity (doted lines) for (a) parallel and (b) perpendicular orientation of RF field and Zeeman field. $\eta = 0.5$ in both cases.

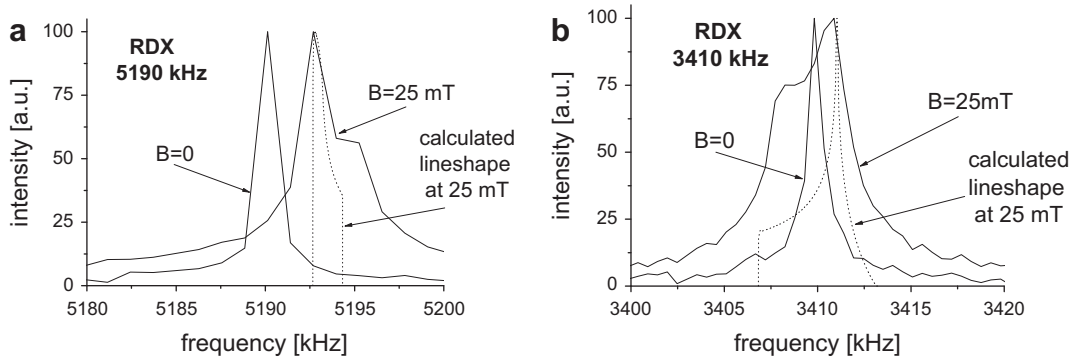

Fig. 5. RDX powder sample at 295 K: the shift and broadening of (a) ν_+ at 5191 kHz and (b) ν_- at 3410 kHz ^{14}N NQR lines in 25 mT magnetic field oriented perpendicular to RF field. The measured lines at $B = 0$ and calculated lines at 25 mT field are also shown. (The low homogeneity of Zeeman field caused additional broadening.)

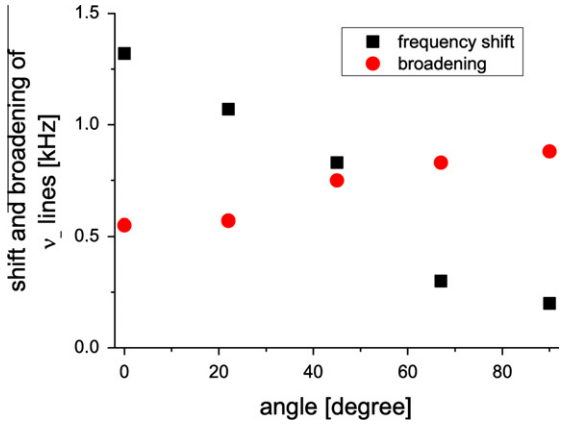

Fig. 6. Angular dependence of frequency shift and line broadening for the average of all three ν_- lines in RDX for different angles between RF and Zeeman field. Angle 0 means RF field is parallel with Zeeman field.

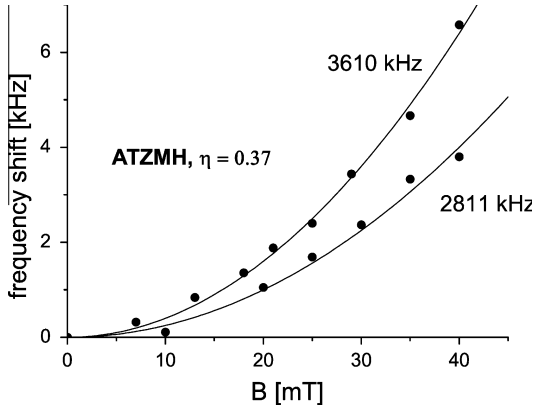

Fig. 7. Frequency shifts vs. applied magnetic field for $\nu_+ = 3610$ kHz and $\nu_- = 2811$ kHz ^{14}N NQR lines in aminotetrazole monohydrate (ATZMH).

is shown in Fig. 6. While we were not able to see any significant orientation dependence in the frequency shift for the ν_+ lines, we noticed that their broadenings were slightly lower for parallel orientation of RF and Zeeman field. In Fig. 4 one can see that the shift of the center of gravity for the ν_- lines is about one order of magnitude bigger than for the ν_+ lines when we move from parallel to perpendicular orientation of RF and Zeeman field. Due to rather low s/n ratio and correspondingly low resolution of NQR signals we have been able to measure only a shift of the centers of gravity of the three averaged ν_- NQR lines in RDX at different angles between RF and Zeeman field shown in Fig. 6.

Similar measurements were performed with aminotetrazole (ATZ)-CH_3N_5 and aminotetrazole monohydrate (ATZMH)-$CH_3N_5H_2O$ [11,12]. The measured results for ATZMH are collected in Table 2.

Again, we observed larger frequency shifts $(\Delta\nu_+ = (\nu_+^*)_{max} - \nu_+)$ for ν_+ transition lines in accordance with expression (7), though ATZMH has a diversity of asymmetry parameters and quadrupole coupling constants. For the pair of ^{14}N NQR lines $\nu_+ = 3610$ kHz and $\nu_- = 2811$ kHz we measured the frequency shift dependence on the applied small Zeeman magnetic field (Fig. 7). The ^{14}N NQR frequency shifts demonstrated a quadratic dependence on magnetic field. This is in agreement with expression (7). Having five different ^{14}N nuclei in the ATZMH molecule, the frequency shift of all five lines in the same Zeeman magnetic field can be compared (Fig. 8). The two groups of measurements, corresponding to five $\Delta\nu_+$ and five $\Delta\nu_-$ frequency shifts of ^{14}N NQR lines in ATZMH follow lines differing in slope by a factor of 2. That follows from expression (7) if one draws $\Delta\nu_+$ and $\Delta\nu_-$ vs. $1/\{Q_{cc}(3+\eta)\}$. The measured points are partly

Table 2
Aminotetrazole monohydrate: the measured ^{14}N NQR transition frequencies, asymmetry parameters, quadrupole coupling constants and frequency shifts in a 20 mT Zeeman magnetic field oriented perpendicular to RF field at 298 K.

ν_+ (kHz)	ν_- (kHz)	ν_0 (kHz)	η	Q_{cc} (kHz)	$\Delta\nu_+$ (Hz)	$\Delta\nu_-$ (Hz)
2732	1490	1242	0.88	2815	3000	2000
3610	2811	799	0.37	4280	1800	1000
3699	2222	1477	0.75	3945	1700	900
3327	2430	897	0.47	3840	1800	800
3141	1928	1214	0.72	3380	2400	1000

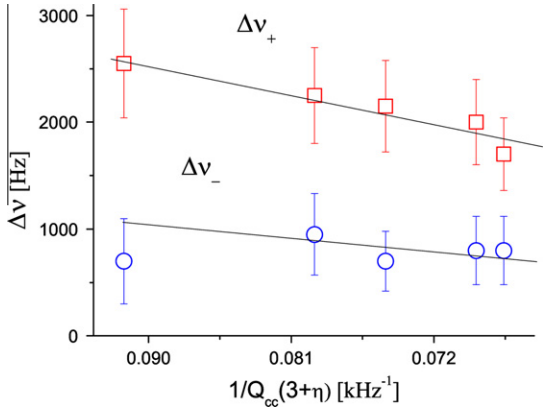

Fig. 8. Comparison of $\Delta\nu_+$ and $\Delta\nu_-$ shifts vs. $1/\{Q_{cc}(3+\eta)\}$ for all five ν_+ and five ν_- ^{14}N NQR transition lines of ATZMH in a 20 mT Zeeman magnetic field.

scattered because the applied field influences the signal intensity and s/n ratio. Namely, for a small applied Zeeman magnetic field the frequency shift is also small and hard to determine because the natural line width of the unperturbed line impedes observation of the much smaller frequency shift. On the other hand, with increase of Zeeman magnetic field the intensities of the shifted lines decrease rapidly due to line broadening.

3. Discussion and conclusions

Due to its ability to identify specific molecules, nuclear quadrupole resonance (NQR), improved in last years, has become a powerful radio-frequency spectroscopic method in basic research in solid state physics and chemistry, as well as in pharmaceutical research and production for nondestructive chemical analysis and polymorph determination. The use in detecting and/or diagnostic application of ^{14}N NQR in identifying different illicit materials, like explosives, narcotics and counterfeit drugs, is becoming more and more important. By adding a small external Zeeman magnetic field to polycrystalline samples we obtained an additional tool which will further increase the identification power of ^{14}N NQR in detection of illicit materials. This is a valuable improvement because searching for unknown NQR frequencies of new substances is often a very time consuming task. Some improvements are known such as the application of the nuclear quadrupole double resonance (NQDR) technique [13]. The advantage of NQDR is its high sensitivity but the resolution is usually low. A possible and faster procedure is to locate the unknown NQR frequencies with the NQDR method first and then to refine the frequency resolution by repeating the measurement with the standard pulse NQR technique and applying polarization enhanced NQR (PENQR) [14] if needed. Unfortunately, in several cases the use of the NQDR method is not possible due to too short proton spin–lattice relaxation time. We were faced with this problem in the study of ^{14}N NQR in ATZ, ATZMH and the pharmaceutically interesting compound famotidine ($C_8H_{15}N_7O_2S_3$) [15]. The common search procedure for unknown NQR resonance lines in such a case is to go step by step over the entire frequency range. If we choose small frequency steps we spend too much time. With larger frequency steps the procedure is faster, but we can overlook some transitions. After finding the NQR transition lines we propose application of small Zeeman magnetic field and measurements of the frequency shifts of all ^{14}N NQR lines found. It is important that the NQR lines are not broadened too much. Using expression (7) and the procedure demonstrated in Fig. 8 we can determine which of NQR lines belong to ν_+ and which to ν_- transitions. This way we also obtained all possible values for ν_0 transitions. The necessary confirmation of ν_0 transitions, ordinary extremely time consuming, because of very low frequencies and correspondingly low s/n ratio, is improved with the suggested technique. In addition, using this technique, we obtained a hint where to continue the search for possibly overlooked NQR lines. The knowledge of NQR lines assignation in similar compounds is also helpful. The NQR line assignation in tetrazole (TZ) [11] was useful for us when studying ATZ and ATZMH.

In conclusion we can say that the suggested application of a small external perturbing Zeeman magnetic field to a powder sample, for which the unknown ^{14}N NQR line pairs ν_+ and ν_- need to be determined, can be of considerable help in some cases in the final assignment of ν_+ and ν_- ^{14}N NQR lines for all nonequivalent nitrogen atoms in a given substance. This technique was proven to be useful in ATZ, ATZMH and famotidine powder samples. Here the double resonance technique could not help us in searching for the unknown ^{14}N NQR lines due to too short proton spin–lattice relaxation time.

Acknowledgment

This work was partially supported by the Grant ARRS J7-9704 from the Slovenian Research Agency.

References

[1] T.P. Das, E.L. Hahn, Nuclear Quadrupole Resonance Spectroscopy, Solid State Physics, Academic Press, New York, 1958. Suppl. 1.
[2] A. Abragam, The Principles of Nuclear Magnetism, Oxford University Press, 1961.
[3] H. Negita, K. Shibata, T. Kubo, ^{14}N Nuclear quadrupole resonances of 2-aminopyrimidine, Bull. Chem. Soc. Jpn. 46 (1973) 110–113.
[4] Y. Morino, M. Toyama, Zeeman effect of the nuclear quadrupole resonance spectrum in crystalline powder, J. Chem. Phys. 35 (1961) 1289–1297.
[5] O. Ege, S. Nishijima, E. Kimura, H. Akiyama, S. Hamai, H. Negita, Powder Zeeman NQR study on the absorption forms for nuclear spin 5/2, Z. Naturforsch. 53a (1998) 314–317.
[6] H.R. Brooker, R.B. Creel, Zeeman nuclear quadrupole resonance line shapes in powders ($I = 3/2$), J. Chem. Phys. 61 (1974) 3658–3665.
[7] K.J. Kim, S.H. Choh, Magnetic resonance of ferroelectric $NaNO_2$, IV. Zeeman effect on ^{14}N nuclear quadrupole resonance in single crystals, J. Kor. Phys. Soc. 17 (1984) 336–339.
[8] V.S. Grechishkin, N.E. Ajnbinder, Nuclear Spin Resonance, Sov. Phys. Uspekhi 6 (1964) 566–587.
[9] R.J. Karpowicz, T.B. Brill, Librational motion of hexahydro-1,3,5-trinitro-s-triazine based on the temperature dependence of the ^{14}N quadrupole resonance spectra, J. Phys. Chem. 87 (1983) 2109–2112.
[10] T.N. Rudakov, V.T. Mikhaltsevich, O.P. Selchikhin, The use of multi-pulse nuclear quadrupole resonance techniques for the detection of explosives containing RDX, J. Phys. D: Appl. Phys. 30 (1997) 1377–1382.
[11] H. Palmer, D. Stephenson, J.A.S. Smith, ^{14}N Quadrupole coupling tensors in solid pyrazole, 1H-1,2,4-triazole and 1H-tetrazole: theory and experiment, Chem. Phys. 97 (1985) 103–111.
[12] J. Pirnat, J. Luznik, V. Jazbinsek, V. Zagar, J. Seliger, T.M. Klapötke, Z. Trontelj, ^{14}N NQR in the tetrazole family, Chem. Phys. 364 (2009) 98–104.
[13] R. Blinc, T. Apih, J. Seliger, Nuclear quadrupole double resonance techniques for the detection of explosives and drugs, Appl. Magn. Reson. 25 (2004) 523–534.
[14] J. Luznik, J. Pirnat, V. Jazbinsek, T. Apih, A. Gregorovic, R. Blinc, J. Seliger, Z. Trontelj, Polarization enhanced "Single Shot" ^{14}N nuclear quadrupole resonance detection of trinitrotoluene at room temperature, Appl. Phys. Lett. 89 (2006) 123509,1–3.
[15] T.J. Humphries, G.J. Merritt, Review article: drug interactions with agents used to treat acid-related diseases, Aliment. Pharmacol. Ther. 13 (3) (1999) 18–26.